

AC MAGNETIC RESPONSE IN (Bi-2223+SrCO₃)/Ag SUPERCONDUCTING TAPES

M. Diantoro^{1,2}, I.M. Sutjahja¹, M.O. Tjia², F. Gömöry³ and P. Kováčik³

¹Jurusan Fisika, Universitas Negeri Malang
Jl. Surabaya 6, Malang 65145

²Jurusan Fisika, Institut Teknologi Bandung
Jl. Ganesha 10, Bandung 40132

³Institute of Electrical Engineering, Slovak Academy of Sciences
Dubravka Cesta, 9, 84239 Bratislava

ABSTRACT

AC MAGNETIC RESPONSE IN (Bi-2223+SrCO₃)/Ag SUPERCONDUCTING TAPES.
A Bi-2223/Ag superconducting tape has been fabricated by means of conventional PIT, followed by eccentric and two axial rolling and heat treatment were introducing an oxide additive (SrCO₃) as a barrier. Temperature dependent of AC magnetic susceptibility measurements have been conducted at various external field B_a . The resulted data were analyzed on the basis of strip model using the wide band approximation. It was found that the imaginary part of the critical current density at 0 K (J_{c0}) is consistently larger than its real part, but both of them tend to decrease with increasing B_a .

Key words : AC magnetic susceptibility, Bi-2223 tapes, SrCO₃ additive.

ABSTRAK

RESPONS MAGNET AC PADA PITA SUPERKONDUKTOR (Bi-2223+SrCO₃)/Ag. Telah dibuat pita superkonduktor Bi-2223/Ag menggunakan metode PIT (*Powder in Tube*) yang dilengkapi proses pengerolan eksentris (*ECR*) dan pengerolan dua-sumbu (*TAR*) serta perlakuan panas yang telah ditambahkan SrCO₃ sebagai barrier. Pengukuran susceptibilitas magnet AC dilakukan pada medan luar B_a yang sejajar permukaan pita dengan nilai berbeda. Analisis data yang diperoleh dilakukan atas dasar model "strip" dalam kerangka rumusan susceptibilitas "wide band". Hasilnya menunjukkan bahwa bagian imajiner dari rapat arus kritis pada 0K (J_{c0}) selalu melebihi bagian realnya, namun keduanya menunjukkan kecenderungan menurun dengan medan B_a yang membesar.

Kata kunci : Susceptibilitas magnet AC, pita superkonduktor Bi-2223, aditif SrCO₃.

INTRODUCTION

AC susceptibility (ACS) measurement has been widely known as a useful means for the study of superconductivity, in particular the vortex state, vortex dynamics and second peak effect [1-4] as well as AC loss and critical current densities [5]. The diamagnetic shielding and the ac losses can be respectively interpreted from the real part $\chi'(T)$ and imaginary part $\chi''(T)$ of the ACS $\chi(T)$ [6]. The shapes of $\chi'(T)$ and $\chi''(T)$ in superconductors are strongly influenced by vortex state, pinning structures, sample morphologies namely bulk, films, wires, tapes, crystals, as well as the measuring conditions [7]. These factors must be duly taken into account in the analysis of the data. Further, interpretation of peaks from ACS measurement can also be used to construct the $H-T$ phase diagram. For BSCCO

tapes, both ACS and resistivity methods have often been used to determine the irreversibility line $H_{irr}(T)$ [8].

The measurement of ACS for superconducting tapes can be carried out with the AC field applied perpendicular to and along the tapes surface. The former is often called strip configuration while the later is named slab configuration. Other important geometrical configuration refers to a disk exposed in perpendicular applied field. The disk model is also often used to approximate the strip one, since these two models exhibit similar behavior with respect to temperature variations.

In the case of thin strip superconducting sample [8,9], one finds that the penetration field B_p , reaches the sample center for the first time is related with the critical current density (J_c) by the expression

$$B_p = \mu_0 J_c h / \pi \dots\dots\dots (1a)$$

where μ_0 and h are vacuum permeability and the thickness of the sample respectively. By the same manner, penetration field for slab and disk configuration may be written respectively as [5]

$$B_p = \mu_0 J_c R \dots\dots\dots (1b)$$

$$B_p = \mu_0 J_c h / 2 \dots\dots\dots (1c)$$

The geometrical parameters used in eqn. 1 a, b, and c are defined in Figure 1. Since μ_0 , h and R are constants, the only intrinsic parameter in the equations is the critical current density J_c , which depends on AC field magnitude (B_a) frequency (ω) and temperature (T). In the case of fixed B_a and ω , temperature dependence of critical current density, J_c is generally expressed as [6]

$$J_c = J_0 \left(1 - \left(\frac{T}{T_c} \right)^m \right)^n \dots\dots\dots (2)$$

where J_{c0} is the critical current density at 0 K, T_c is critical superconducting temperature, while m and n are model dependent exponents.

The expression of complex ACS has been derived with the real and imaginary parts given by [5].

$$\chi' = \frac{4}{\pi y} \int_0^\pi \cos \theta \cdot \tanh \left[y \cdot \sin^2 \left(\frac{\theta}{2} \right) \right] \cdot d\theta \dots\dots\dots (3)$$

$$\chi'' = \frac{4}{\pi y} \left[\frac{2}{y} \ln(\cosh y) - \tanh y \right]$$

with the variable y relates the AC field amplitude to the penetration field, by $y = B_a / B_p$. The above expressions can be simplified by means of the related wide band formulation [5]. According to this scheme, the real part corresponds to the sample magnetization at maximum AC field and the imaginary part is linked to remnant magnetization, which are denoted by $\chi_a(T)$ ($T, \omega t = 0$) and $\chi_r(T, \omega t = \pi/2)$ respectively. The resulting mathematical expressions for strip model are now reduced to the simple form

$$\chi_a = -\frac{1}{y} \tanh y \dots\dots\dots (4)$$

$$\chi_r = -\frac{1}{y} \left[\tanh y - 2 \tanh \left(\frac{y}{2} \right) \right]$$

Following the same formulation, the wide band ACS for slab gives

$$\chi_a = \begin{cases} y/2 - 1 \\ -1/2 y \end{cases} \dots\dots\dots (5)$$

$$\chi_r = \begin{cases} y/4 \\ 1 - y/4 - 1/2 y \\ 1/2 y \end{cases}$$

while the expressions for the disk model are

$$\chi_a = \frac{1}{2y} \left[a \cos \left(\frac{1}{\cosh y} \right) + \frac{\sinh y}{\cosh^2 y} \right] \dots\dots\dots (6)$$

$$\chi_r = -\frac{1}{2y} \left[a \cos \left(\frac{1}{\cosh y} \right) + \frac{\sinh y}{\cosh^2 y} \right] + \frac{1}{y} \left[a \cos \left(\frac{1}{\cosh y} \right) + \frac{\sinh \frac{y}{2}}{\cosh \frac{y}{2}} \right]$$

For clarity we define the notations used for describing the dimensions of each model as depicted in Figure 1.

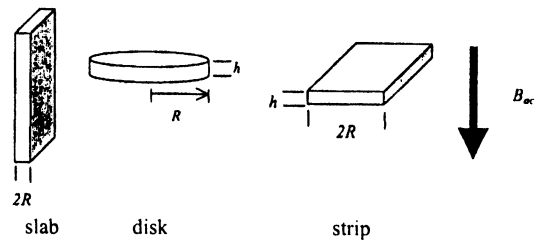


Fig. 1. The sample shape configuration along with the definition of notations used in the calculation and data analysis.

We present in this report the result of ACS measurements for a small cut of tape sample in external field applied perpendicular to the wide tape surface. As a consequence, the model of thin superconducting strip is used in the data analysis. For comparison, calculated AC magnetic susceptibilities for the three models discussed above are also presented in this paper.

EXPERIMENTAL

Superconducting tape of BSCCO-2223 sample have been prepared by means of conventional powder in tube (PIT) method. The superconducting core consists mainly of dominantly 2212 phase of Bi_{1.6}Pb_{0.4}Sr₂Cu₂CU₃O₁₀₊₂. Powder with a small amount of

SrCO₃ (10% of weight) additive has been added prior to PIT process. The filled tube was first sintered and then drawn thermomechanically followed by two axial rolling (TAR) and eccentric rolling to produce better grain arrangement. The resulted tape was again heated for annealing treatment. The physical dimension of the resulted tape was about 3.41 mm x 1.89 mm x 1.5 m. We used the same sintering and annealing temperature of about 835 °C. Detail of sample preparation is explained elsewhere [10, 11].

An X-ray diffraction was performed to a small cut of the sample using Cu-K α radiation source after appropriate etching of one side of the surfaces. In the AC magnetic measurement, the frequency was set at 21 Hz with a field strength of 0.02, 0.1, 0.5 and 2.5 mT. Since the crystals in these tapes are mainly oriented parallel to the surface in this case, B_a is practically parallel to c crystallographical axis. The setting and performance of the equipment is explained in Ref [5].

RESULT AND DISCUSSIONS

The result of X-ray diffraction pattern obtained from a constant wavelength (Cu-K α) Bragg-Brentano diffractometer is depicted in Fig 2. The diffraction pattern shown in the figure consists of strong peaks associated with (001) plane of Bi-2223 and weak peaks belonging to the (008) and (0012) signals of Bi-2212. This result confirms that the c crystallographical axis is mostly perpendicular to the tape surface. Given in the inset is a result of analysis obtained by using Cell Ref [12] in the frame of $CmCm$ space group with the lattice parameters the a , b and c given respectively by 5.399 Å, 5.410 Å and 37.100 Å according to Ref. [13], while Bi-2212 phase contributions associated with (008) and (0012) peaks are identified on the basis of $Fmmm$ space group [14]. The high crystal quality is readily demonstrated by the narrow width of the peak and the flat back ground.

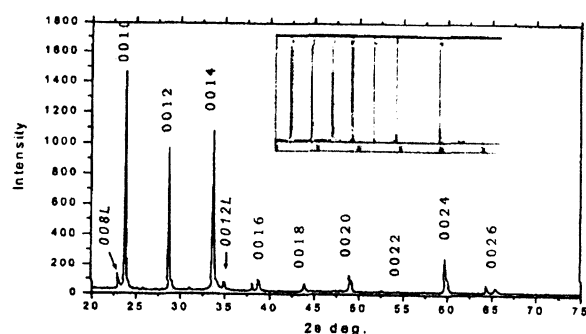


Fig. 2. Profile of X-RD using Cu-K α constant wavelength. The exclusive occurrence of (001) peaks in the figure reflects a very highly oriented Bi-2223 phase of the grains. Two weak impurity peaks are also identified as (008) and (0012) of Bi-2212 phase. The narrow width of the peaks and the very flat background reveals a high crystal quality.

The temperature dependent AC magnetic responses for the three different models of superconductors are displayed in Fig. 3. We assumed in the calculation the same critical temperature 108.2 K and critical current density 5×10^8 A-m² for all three cases. The dimensions used were 1.04 mm x 3.4 mm ($h \times 2R$) for strip, 1.04 mm x 3.4 mm ($h \times R$) for cylindrical disk and 1.04 mm ($2R$) for slab configurations. For the strip and disk, the external AC field B_a applied perpendicular to the broad surface as shown in the Fig. 1, was chosen to be 0.5 mT.

As displayed in the Fig. 2 the responses of those three different configurations differ in both the real and imaginary parts. The real parts for the disk and strip models show roughly the same trend, while that of the slab model appears to depend on the temperature more sensitively. The magnitude of Meissner screening effect measured by χ' increases from the slab, disk to the strip configuration successively. In conjunction to the real parts, the related imaginary parts χ'' also exhibit the same pattern of temperature variation. The peak positions (T_p) are also shifted to a successively higher temperature in the order of the slab, disk and strip model.

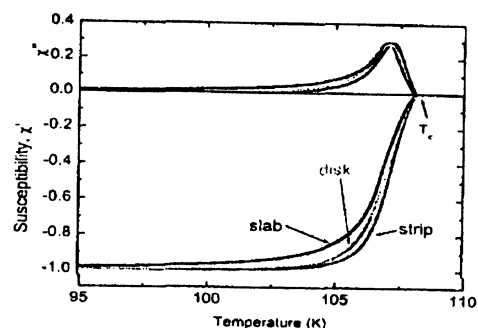


Fig. 3. Calculated real and imaginary parts of AC magnetic responses for three different models. From left to right are plots for slab, disk and strip model respectively.

As mentioned earlier, our experimental setting is best described by the strip configuration. We have therefore analyzed the data on the basis of this model. The data of the sample obtained in the four different

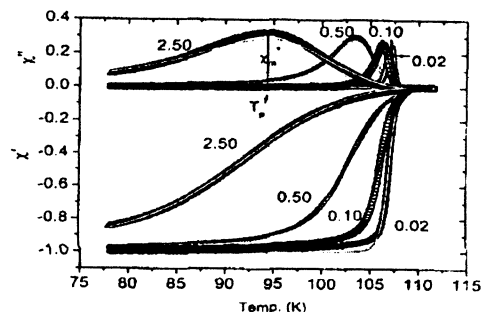


Fig 4. Plots of AC magnetic response (susceptibility) χ' and χ'' of various ac field (symbols) and the resulted best fit according to the strip model (lines). Temperature peak position, T_p and associated peak maximum, χ_m are also displayed.

applied fields in this experimental is presented in Figure 4. For the analysis of these data, the real and imaginary parts are handled separately, using eqn, 1a, 2 and 4 by setting $m = 1$ following our previous choice [15] while leaving n , T_c and J_{c0} as free parameters. The results of best fit are shown in Fig. 4 along with ACS data, and the corresponding parameters are given in Table 1, except

Table 1. Set of parameters inferred from fitting procedures. Data fitted well under a reasonable statistical of R^2 and χ^2 values. The unit of J_{c0} is 10^8 A m^2 for both Real and Imaginary parts. AC field is written in 10^{-3} T.

| Field | Real | | | | Imaginary | | | |
|-------|----------|-------|-------|----------|-----------|-------|-------|----------|
| | J_{c0} | n | R^2 | χ^2 | J_{c0} | n | R^2 | χ^2 |
| 0.02 | 7.411 | 1.786 | 0.99 | 0.0005 | 12.111 | 1.586 | 0.97 | 0.0001 |
| 0.10 | 6.949 | 1.726 | 0.99 | 0.0009 | 11.908 | 1.582 | 0.98 | 0.0001 |
| 0.50 | 5.171 | 1.544 | 0.99 | 0.0004 | 8.486 | 1.549 | 0.98 | 0.0002 |
| 2.50 | 5.075 | 1.501 | 0.99 | 0.0008 | 6.556 | 1.563 | 0.96 | 0.0004 |

the value of T_c which turns out to be practically the same ($T_c = 108.20$ K) in all cases. It is clear from the Table, that J_{c0} decreases with increasing external field as expected on general ground. Further, we note that the imaginary part of J_{c0} is consistently larger than its real parts, while the associated n values appear to remain more or less independent of field for the imaginary part. It is found that the strip model gives reasonably good fit to tile data in most cases within our experimental rage as indicated by the associated R^2 and χ^2 values.

CONCLUSION

An Ag sheathed superconducting tape with highly oriented crystal of (Bi2223 +SrCO₃) has been successfully fabricated. The AC magnetic responses for the strip, disk and slab configuration have been discussed in the frame work of wide band susceptibility formulation, with the strip model adopted for our data analysis in according to the experimental setting. As the result of the fitting, we obtained the values of T_c , J_{c0} and n , as well as the variations of the last two parameters with the external field.

ACKNOWLEDGEMENT

Part of this work was supported by RUT V (207/SP/RUT/BPPT/IV/97), VEGA (2/6056/99), EU (GSRD-CT-1 999-00049) and KNAW projects. One of us (MD) wishes to thanks I. Hušek for sample preparation and J. šouc for experimental set up.

REFERENCES

- [1]. M.J. QIN AND X. X YAO, *Physical Review B* **54**(10)(1996-11) 7536
- [2]. D. LEBLAC AND M.A.R. LEBLAC, *Physical Review B* **45**(10)(1992) 5443.
- [3]. K.C.HUNG, C. C. LAM, X. JIN, J. FENG AND H. M. SHAO, *Physica C* **280** (1997) 317
- [4]. D. MARTEIN, Quantum Design, "Introdziction to AC Susceptibility", San Diego, USA,
- [5]. F. GOMORY, L. GHERARDI, R. MELE, D. MORIN, G. CROTTI, *Physica C* **279** (1997) 39
- [6]. S. ÇELEBI, *Physica C* **316** (1999) 251
- [7]. G.C. HAN, C.K. ONG, *Physica C* **311**(1999) 29
- [8]. E. H. BRANDT, *Physical Review B* **49** (13) (1994) 9024.
- [9]. F. GOMORY, I. HUSEK, P. KOVAC, and L. KOPERA, in "Studies of High Temperature Superconductors" Vol. 32, Ed. A. V. tiai-likar
- [10]. M. DIANTORO, M.O. TJIA, I. HUSEK, and P. KOVÁÈ, *Physica C* **357** (2001)1182
- [11]. P. KOVÁÈ, I. HUSEK, A. ROŠOVA, W. PACHIA, *Physica C* **312** (1999) 179-190.
- [12]. B. BOCHU AND J. LAGUER, CellRef v3.0, *Manual and Software*, INPG, France (2001).
- [13]. D.Y. Li, B.H. O'CONNOR, A. VANRIESEN, L. W. MACKINNON, D. J. COOKSON, R.F. GIRRET and B. A., FLUNTER, *Denver X-Ray Conference* (1996).
- [14]. S. A. SUNSHINE, T. SIEGRIST, L. F. SCHEEMEYER, D. W., MURPHY, R.J. CAVA, B. BATIÖG, R. B. VANDOVER, R. M. FLEMMING, S. H. GLARUM, S. NAKAHARA, R. FARROW, J.J. KRAJEWSKI, S. M. ZAHURAK, J. V. WASZCZAK, P.MARSLI, L. W. RUPP JR. and W. F. PECK, *Phys. Rev. B* **38** (1988).
- [15]. M. DIAITORO, W. LOCKSINANTO, M. O. TJIA, F. GOMORY, J. SOUC, I. HUSEK and P. KOVAC, presented in 14'h International Symposium on Superconductivity, ISS 25 - 27 September, KOBE Japan (2001), submiotted to *Physica C*.